DR. CLAIRE XI ZHANG (Orcid ID : 0000-0002-4687-039X)

Article type : Original Article

Synaptotagmin-11 inhibits spontaneous neurotransmission through vti1a

Wan-Ru Li[1*], Ya-Long Wang[1*], Chao Li[2,3*], Pei Gao[1], Fei-Fan Zhang[1], Meiqin Hu[4], Jing-Chen Li[1], Shuli Zhang[2,3], Rena Li[5], Claire Xi Zhang[1,6]

1 Beijing Institute of Brain Disorders, Laboratory of Brain Disorders, Ministry of Science and Technology, Collaborative Innovation Center for Brain Disorders, Capital Medical University, Beijing, China

2 State Key Laboratory of Brain and Cognitive Sciences, Institute of Biophysics, Chinese Academy of Sciences, Beijing, China

3 University of Chinese Academy of Sciences, Beijing, China

4 Department of Molecular, Cellular, and Developmental Biology, University of Michigan, Ann Arbor, MI, USA

5 Beijing Key Laboratory of Mental Disorders, Beijing Anding Hospital and Beijing Institute of Brain Disorders, Capital Medical University, Beijing, China

6 Academy of Pharmacy, Xi'an Jiaotong-Liverpool University, Suzhou, China

Correspondence

Rena Li

Beijing Key Laboratory of Mental Disorders, Beijing Anding Hospital and Beijing Institute of Brain Disorders, Capital Medical University, Beijing, China.

E-mail: renali@ccmu.edu.cn

Claire Xi Zhang
Beijing Institute of Brain Disorders, Laboratory of Brain Disorders, Ministry of Science and Technology, Collaborative Innovation Center for Brain Disorders, Capital Medical University, Beijing, China.
E-mail: clairexizhang@ccmu.edu.cn
*WRL, YLW, and CL contributed equally to this work.

Abstract

Recent work has revealed that spontaneous release plays critical roles in the central nervous system, but how it is regulated remains elusive. Here we report that synaptotagmin-11 (Syt11), a Ca^{2+}-independent Syt isoform associated with schizophrenia and Parkinson's disease, suppressed spontaneous release. Syt11-knockout hippocampal neurons showed an increased frequency of miniature excitatory postsynaptic currents while overexpression of Syt11 inversely decreased the frequency. Neither knockout nor overexpression of Syt11 affected the average amplitude, suggesting the presynaptic regulation of spontaneous neurotransmission by Syt11. Glutathione-S-transferase pull-down, co-immunoprecipitation, and affinity-purification experiments demonstrated a direct interaction of Syt11 with vps10p-tail-interactor-1a (vti1a), a non-canonical SNARE protein that maintains spontaneous release. Importantly, knockdown of vti1a reversed the phenotype of Syt11 knockout, identifying vti1a as the main target of Syt11 inhibition. Domain analysis revealed that the C2A domain of Syt11 bound vti1a with high affinity. Consistently, expression of the C2A domain alone rescued the phenotype of elevated spontaneous release in Syt11-knockout neurons similar to the full-length protein. Altogether, our results suggest that Syt11 inhibits vti1a-containing vesicles during spontaneous release.

Keywords synaptotagmin, vti1a, spontaneous release, SNARE

Abbreviations

eEPSCs evoked excitatory postsynaptic currents

FL full-length

GST Glutathione S-transferase

KD knockdown

KO knockout

mEPSCs miniature excitatory postsynaptic currents

NT non-targeting shRNA

OE overexpression

PI protease inhibitor cocktail

sEPSCs spontaneous excitatory postsynaptic currents

syb2 synaptobrevin2

Syt11 synaptotagmin-11

TTX tetrodotoxin

vti1a vps10p-tail-interactor-1a

Introduction

Spontaneous neurotransmission at the frog neuromuscular junction was initially discovered by Fatt and Katz about 70 years ago (Fatt & Katz 1950; Fatt & Katz 1952). Since then, it has been found in every type of synapse under physiological conditions in which neurotransmitter is released at a low frequency. Accumulating evidence points to important functions of spontaneous release, including postsynaptic signal transduction, guiding the maturation of primeval synapses, and mediating synaptic plasticity (Kavalali 2015).

The molecular mechanisms underlying spontaneous release are less well understood than action potential-evoked release and it has been a long-standing question as to whether and how they are related (Kaeser & Regehr 2014; Truckenbrodt & Rizzoli 2014). Considerable evidence supports the idea that they are driven by either the same vesicle pool or separate pools (Sara *et al.* 2005; Groemer & Klingauf 2007; Mathew *et al.* 2008; Ikeda & Bekkers 2009; Fredj & Burrone 2009; Hua *et al.* 2011; Cornelisse *et al.* 2012). Recent studies have revealed some molecular distinctions between these two types of neurotransmission (Kavalali 2018;

Gonzalez-Islas *et al.* 2018; Andreae & Burrone 2018; Williams & Smith 2018). While evoked and spontaneous neurotransmission are predominantly mediated by the canonical SNARE complex comprising synaptobrevin2 (syb2, also named VAMP2), syntaxin1, and SNAP-25 (Sudhof & Rothman 2009), some of the spontaneous neurotransmitter release is mediated by alternative vesicular SNARE proteins, such as VAMP7, vps10p-tail-interactor-1a (vti1a), and to some degree VAMP4 (Hua *et al.* 2011; Raingo *et al.* 2012; Ramirez *et al.* 2012; Bal *et al.* 2013; Crawford *et al.* 2017; Kononenko & Haucke 2012). Among them, vti1a is trafficked most robustly at rest and promotes high-frequency spontaneous release (Ramirez *et al.* 2012). Loss of both syb2 and vti1a markedly diminishes high-frequency spontaneous neurotransmission, suggesting that syb2- and vti1a-containing vesicles are mainly responsible for spontaneous release. Vti1a belongs to a family of SNARE proteins that regulate endolysosomal trafficking and are conserved from yeast to human (Emperador-Melero *et al.* 2019). Vti1a and vti1b, mammalian genes universally expressed in all tissues (Advani *et al.* 1998), play largely redundant roles in regulating protein sorting at the Golgi, and they are also required for synaptic transmission and dense-core vesicle secretion (Walter *et al.* 2014; Emperador-Melero *et al.* 2018; Emperador-Melero *et al.* 2019). Vti1a, but not vti1b, is localized at synapses and in synaptic vesicle fractions (Antonin *et al.* 2002; Takamori *et al.* 2006), supporting its unique role in spontaneous neurotransmission (Ramirez *et al.* 2012; Crawford *et al.* 2017; Kononenko & Haucke 2012).

Besides the molecular distinction in the SNARE complex, spontaneous neurotransmission is also differentially regulated by SNARE-binding proteins (such as synaptotagmins, complexin, double C2-domain containing protein, and copine6), neuromodulators, and other signaling pathways compared to evoked neurotransmitter release (Maximov & Sudhof 2005; Glitsch 2006; Huntwork & Littleton 2007; Xu *et al.* 2009; Groffen *et al.* 2010; Pratt *et al.* 2011; Pang *et al.* 2011; Yang *et al.* 2013; Fawley *et al.* 2014; Schupp *et al.* 2016).

In this study, we investigated the function of synaptotagmin-11 (Syt11), a Ca^{2+}-independent syt isoform essential for mouse development (von Poser *et al.* 1997;

Shimojo *et al.* 2019), in spontaneous neurotransmission. Syt11 is a risk locus for Parkinson's disease and a candidate gene for susceptibility to schizophrenia (Huynh *et al.* 2003; Inoue *et al.* 2007; International Parkinson Disease Genomics *et al.* 2011; Pihlstrom *et al.* 2013; Sesar *et al.* 2016). It belongs to the syt family, which is known for its roles in evoked and/or spontaneous neurotransmission (Pang & Sudhof 2010). Syt1, Syt2, and Syt9 all act as Ca^{2+} sensors to promote evoked neurotransmission but clamp spontaneous release (Maximov & Sudhof 2005; Xu *et al.* 2009; Xu *et al.* 2007; Geppert *et al.* 1994; Nishiki & Augustine 2004; Pang *et al.* 2006; Sun *et al.* 2007; Liu *et al.* 2009; Bacaj *et al.* 2013; Wierda & Sorensen 2014). Syt4, which is most homologous with Syt11 and does not bind Ca^{2+} biochemically either, suppresses spontaneous release without affecting evoked exocytosis (Dean *et al.* 2009). In contrast, Syt12, also a non-Ca^{2+} binding Syt, selectively promotes spontaneous release, leaving evoked neurotransmission unaltered (Maximov *et al.* 2007). Therefore, different Syt family members play distinct roles in spontaneous release, most likely due to unique protein-protein and/or protein-lipid interactions. Syt11 plays multiple roles in membrane trafficking in neurons and glia (Wang *et al.* 2016; Bento *et al.* 2016; Sreetama *et al.* 2016; Du *et al.* 2017; Wang *et al.* 2018; Shimojo *et al.* 2019; Yan *et al.* 2020). It regulates neuronal endocytosis, the autophagy-lysosome pathway, and synaptic plasticity; functions in lysosome exocytosis for membrane repair, caveolae-mediated endocytosis, and mechanoprotection in astrocytes; and inhibits phagocytosis and cytokine release in microglia. We previously reported that Syt11 inhibits clathrin-mediated and bulk endocytosis without affecting evoked exocytosis (Wang *et al.* 2016). Recently, Shimojo *et al.* reported that Syt11 does not regulate evoked neurotransmission, and does not bind the canonical SNARE complex (Shimojo *et al.* 2019). Interestingly, a study of Syt11-interacting partners in β-cells showed that vti1a can be pulled down by glutathione-S-transferase (GST)-Syt11 (Milochau *et al.* 2014). Therefore, we hypothesized that Syt11 may regulate spontaneous release *via* vti1a-containing vesicles.

Materials and methods

1. Reagents

The primary antibodies for Western blots, immunofluorescence and co-immunoprecipitation assays were anti-Syt11 (Synaptic Systems Cat# 270003, RRID: AB_2619994, working dilution: 1:500-1000), anti-Syb2 (Synaptic Systems Cat# 104211, RRID: AB_887811, 1:1000), anti-Vti1a (BD Biosciences Cat# 611220, RRID: AB_398752, 1:1000), anti-c-Myc (Santa Cruz Biotechnology Cat# sc-42, RRID: AB_2282408, 1:5000), mouse normal IgG (Millipore Cat# 12-371, RRID: AB_145840, 1:250), rabbit normal IgG (Millipore Cat# 12-370, RRID: AB_145841, 1:250), anti-GAPDH (Sigma-Aldrich Cat# G8795, RRID: AB_1078991, 1:10000), and anti-His (Absin Bioscience Inc., Cat# 830002 (2019), 1:1000). All cell culture media were from Hyclone (Logan, UT). Chemicals were from Sigma unless stated otherwise.

2. Animals

The floxed Syt11 knock-in mice were from The Jackson Laboratory (stock number 008294, strain B6.129-Syt11$^{tm1Sud/J}$, purchased in 2011). This strain was genotyped using the specific forward primer 5'-AATCTCAGCACTCAGGAGTCAG-3' and reverse primer 5'-CTCTTGCTTACTGATTGGCAGC-3'. PCR was performed at an annealing temperature of 57°C (1 min) and extension at 72°C (1 min) for 35 cycles. The Syt11 knock-in homozygote showed a 500-bp band and wild-type mice a 361-bp band. The Syt11 gene was silenced using cre recombinase. The animals were housed with free access to food and water *ad libitum*. The care and use of animals was approved and directed by the Animal Care and Use Committee of Capital Medical University (protocol# AEEI-2015-124). The study was not pre-registered. Neither randomization nor blinding was performed in this study.

3. Cell Culture

Hippocampi were dissected from 1- to 2-day-old floxed Syt11 knock-in mice or C57BL/6 mice under hypothermia. Neurons were dissociated with trypsin (0.25 mg/ml for 15 min at 37°C), then triturated with a 2-ml Pasteur pipette, and plated on 2.5-cm coverslips coated with poly-D-lysine (Sigma-Aldrich Cat# 0899 (2017)). One mouse was used for every three coverslips. The culture medium consisted of 96%

178 Neurobasal-a, 2% B-27 supplement, and 2% Glutamax. Cultures were maintained at
179 37°C in a humidified incubator gassed with 95% air and 5% CO_2. All cultured neuron
180 experiments were performed at 14-16 days *in vitro* (DIV).

181 **4. Lentiviral Preparation**

182 Lentivirus was prepared by transfecting the pFUGW plasmid with genes of interest
183 and three helper plasmids pRev, pRRE, and pVSVG (expressing viral packaging and
184 coating proteins) into human embryonic kidney (HEK) 293-T cells (ATCC® Cat#
185 CRL-3216™, RRID: CVCL_0063) (this cell line is not listed as a commonly
186 misidentified cell line by the International Cell Line Authentication Committee). No
187 further authentication was performed in the laboratory. A maximum of 5 cell passages
188 was used. The virus was harvested from the culture medium 48 h after transfection.
189 Primary cultured hippocampal neurons were infected with lentivirus at DIV4 or twice
190 at DIV4 and DIV5. The infection efficiency was ~90%.

191 The cre- and Δcre-expressing lentivirus plasmids were a kind gift from Dr. Chen
192 Zhang (Capital Medical University). They contained enhanced green fluorescent
193 protein (EGFP) followed by a nuclear localization signal (NLS) and the cre or Δcre
194 recombinase sequence (EGFP-NLS-CRE/ ΔCRE).

195 The hairpin shRNA sequences used to knock down vti1a in primary cultured
196 hippocampal neurons were as follows: sense 5'-GGGCACATCTGCTGGATAA-3'
197 (vti1a KD-1) and sense 5'-GCAGTGGAGACTGAGCAAA-3' (vti1a KD-2). A
198 random sequence (sense 5'-TTCTCCGAACGTGTCACGT-3') that was predicted not
199 to target any genes in mouse cells served as a negative control (Shanghai Obio
200 Technology Corp., Ltd.).

201 For overexpression and rescue experiments, lentivirus expressing
202 myc-Syt11-IRES2-BFP or myc-C2A-IRES2-BFP was used. Three copies of c-myc
203 tag (GAGCAGAAGCTGATCAGTGAAGAGGACTTG in the DNA sequence) and a
204 linker region (GGCAGCGGTAGT) were tagged to the N-terminal of the mouse
205 Syt11 gene.

206 **5. Electrophysiology**

207 All data were acquired by a HEKA USB10 amplifier and PatchMaster software

(Lambrecht/Pfalz, HEKA USB10, RRID: SCR_000034). For mEPSC recording, the external bath solution contained (in mM) 150 NaCl, 4 KCl, 2 $MgCl_2$, 2 $CaCl_2$, 10 glucose, and 10 HEPES (pH 7.4, adjusted with NaOH). For isolation of miniature EPSCs (mEPSCs), tetrodotoxin (TTX, 1 μM) (Apexbio Cat# N1671 (2017)) and the $GABA_A$ receptor blocker bicuculline (20 μM) (Selleck Cat# s7071 (2017)) were added. The pipette solution contained (in mM) 135 CsCl, 10 HEPES, 1 EGTA, 1 Na-GTP, 4 Mg-ATP, and 10 QX-314 (Alomone Labs Cat# Q100Q16500 (2017)) (pH 7.4, adjusted with CsOH). All the mEPSC events were recorded at a holding potential of −70 mV. Pipettes (Sutter Instrument Cat# BF-150-110-10HP (2017)) used in recording had a resistance of 3-5 MΩ. Neurons with a leak current >200 pA were discarded. mEPSC frequencies were analyzed by Mini Analysis Software (RRID: SCR_002184) (search parameters: gain: 20; blocks: 3940; threshold (pA): 20; period to search for a local maximum (μs): 20000; time before a peak for baseline (μs): 5000; period to search a decay time: 5000; fraction of peak to find a decay time: 0.5; period to average a baseline (μs): 2000; area threshold: 10; number of points to average for peak: 3; direction of peak: negative).

For evoked EPSC recording, pipettes were filled with a solution containing (in mM): 120 $CsMeSO_4$, 10 HEPES, 10 EGTA, 4 Na_2-ATP, 1 Na_3-GTP, 2 $MgCl_2$, 4 QX-314 (pH 7.32–7.36; osmolarity 294–298). AMPAR-EPSCs were recorded in whole-cell voltage-clamp mode at a holding potential of –70 mV using artificial cerebrospinal fluid containing 0.1 mM picrotoxin (Tocris Cat# 1128 (2018)). Evoked synaptic currents were elicited by afferent fiber stimulation with a concentric bipolar electrode (FHC Cat# 211386 (2018)) and controlled by a Model 2100 Isolated Pulse Stimulator (A-M Systems, Inc., RRID: SCR_016677). We gradually adjusted the stimulus intensity to ensure the maximum EPSC amplitude and to avoid the extra disturbance from eliciting multiple action potentials. Paired-pulse eEPSC ratios were recorded from the same hippocampal neurons at interpulse intervals of 50 ms (20 Hz), 100 ms (10 Hz), 200 ms (5 Hz), and 500 ms (2 Hz) (Regehr 2012; Hu *et al.* 2021). Spontaneous EPSCs (sEPSCs) were recorded from the same hippocampal neurons 1 min after the paired-pulse stimulation.

238 **6. GST pull-down assay**

239 The GST-Syt11 plasmid was constructed by inserting the cytosolic region
240 (amino-acids 37–428) of Syt11cDNA (AF000423) into the pGEX4T2 vector with a
241 linker sequence of LVPRGSPGIP at its N-terminal. Proteins were induced by 0.2 μM
242 IPTG at room temperature for 5 h and purified with GST Glutathione Sepharose™ 4B
243 beads (GE Healthcare Cat# 17-0756-01 (2018)). Briefly, bacterial pellets from 200 ml
244 LB culture medium were suspended in 10 ml lysis buffer (50 mM NaH_2PO_4, 300 mM
245 NaCl, pH 8.0) containing 1 mg/ml lysozyme, 1×PI (protease inhibitor cocktail, Roche
246 Cat# 04693132001 (2018)), and 1 mM phenylmethylsulfonyl fluoride (PMSF). The
247 cells were lysed for 30 min on ice and sonicated. Then, after centrifugation at 20,000
248 *g* for 15 min, the supernatant was incubated with 200 μl Glutathione Sepharose™ 4B
249 beads at 4°C for 5 h. After 3 washes in phosphate-buffered saline (PBS), the
250 concentration of GST-tagged proteins immobilized on beads was quantified by
251 Coomassie staining of SDS PAGE gels and the beads were stored at 4°C for further
252 experiments.

253 Mice were anesthetized using isoflurane and rapidly decapitated. The brains were
254 homogenized in lysis buffer (20 mM Tris (pH 7.5), 150 mM NaCl, 1% Triton X-100,
255 1 mM EDTA, 1×PI, and 1 mM PMSF and rotated at 4°C for 2 h. After centrifugation
256 for 15 min at 20,000 *g* at 4°C, 2 mg of total proteins was collected in the supernatant
257 and pre-cleared for 1 h at 4°C with 20 μg Glutathione Sepharose™ 4B beads. After a
258 quick spin, the supernatant was incubated with 20 μg of immobilized GST fusion
259 protein on Glutathione Sepharose™ 4B beads at 4°C for 4 h. The resin was collected
260 after a quick spin and underwent five washes with lysis buffer, followed by treatment
261 with SDS sample buffer at 65°C for 10 min for Western blotting.

262 **7. Co-immunoprecipitation**

263 Co-IP was performed with 4 μg anti-vti1a antibody and its corresponding isotype IgG
264 antibody. The mouse brain lysate (prepared in 20 mM Tris (pH 7.5), 500 mM NaCl,
265 1% Triton X-100, 1 mM EDTA, 1×PI, and 1 mM PMSF) was incubated with
266 anti-vti1a antibody at 4°C overnight followed by 40 μl protein G Sepharose beads.
267 After three washes with lysis buffer, the beads were treated with SDS sample buffer at

65°C for 10 min before Western blotting.

8. Purified protein-binding assays *in vitro*

The GST-Syt11 mutants contained the following amino-acid sequences: linker (37–156), Δlinker (157–428), C2A (157–290), ΔC2A (37–156 and 291–428), C2B (291–428), and ΔC2B (37–290). They were inserted into the pGEX4T2 vector the same as GST-Syt11.

The His-vti1a plasmid was constructed by inserting the cDNA of vti1a (NM_001293685.1) into the bacterial protein expression vector pET with a 6xHis tag at its N-terminal (pET-6xHis/mVti1a).

The bacterial pellets from 200 ml culture medium were suspended with 10 ml lysis buffer (50 mM NaH_2PO4, 300 mM NaCl, pH 8.0) containing 1 mg/ml lysozyme, PI, and 1 mM PMSF. The cells were lysed for 30 min on ice and sonicated. To purify His-tag proteins, the centrifuged supernatant was incubated with 1 ml His-tag purification resin (Beyotime Cat# P2218 (2019)) at 4°C for 1 h. The lysate was transferred to an Ni column, and washed 3 three times with washing buffer (in mM: 50 NaH_2PO4, 300 NaCl, 2 imidazole, pH 8.0). The bound proteins were eluted with elution buffer (in mM: 50 NaH_2PO4, 300 NaCl, 50 imidazole, pH 8.0).

The binding essay was performed according to Yan *et al.* (Yan *et al.* 2020) with modifications. Briefly, purified GST-Syt11 and mutants (immobilized on Glutathione Sepharose™ 4B beads) were incubated with His-vti1a protein (2.5 μM) in 500 μl of reaction buffer (50 mM Tris-HCl, 100 mM NaCl, 0.5% Triton X-100, pH 8.0) at 4°C for 1 h. The bound fraction was washed five times with washing buffer (50 mM Tris-HCl, 150 mM NaCl, 0.5% Triton X-100, pH 8.0) and Western blotting was performed.

9. Immunofluorescence

Immunofluorescence experiments were performed as in Du *et al.* (Du *et al.* 2017). Briefly, neurons were fixed in 4% paraformaldehyde and quenched in 1 mg/ml $NaBH_4$ in TBS (in mM: 20 Tris pH 7.5, 154 NaCl, 2 EGTA, 2 $MgCl_2$). The cells were then blocked in TBS containing 2% bovine serum albumin and 0.02% saponin and treated sequentially with primary and secondary antibodies. The mounted cells were

imaged under a Leica TCS SP8 confocal microscope with a 63× objective and 2.5× digital zoom. Co-localization was analyzed using the Pearson's coefficient plug-in in NIH ImageJ (RRID: SCR_003070).

10. Western blotting

Western blotting experiments were performed as in Wang *et al.* (Wang et al. 2016). In brief, cells were washed with PBS and suspended on ice in lysis buffer (20 mM Hepes, 100 mM KCl, 2 mM EDTA, 1% NP-40, 1 mM PMSF, and 1×PI, pH 7.4). After centrifugation at 15000 *g* for 15 min at 4°C, the supernatants were collected and boiled in SDS-PAGE buffer. Proteins were separated on 10% SDS-polyacrylamide gels and transferred to nitrocellulose filter membranes. Each membrane was blocked for 1 h in PBS containing 0.1% Tween 20 (v/v) and 5% nonfat dry milk (w/v). After washing 3 times with 0.1% Tween 20 containing PBS (PBST), the blots were incubated with primary antibodies at 4°C overnight in PBST containing 2% bovine serum albumin and secondary antibodies at room temperature for 1 h. Blots were scanned with an Odyssey infrared imaging system (LI-COR Biosciences, RRID: SCR_014579) and quantified with ImageJ.

11. Statistical analysis

All experiments were independently replicated at least three times. Data are shown as the mean ± SEM. Results were analyzed using GraphPad Prism 7.0 software (RRID: SCR_002798). The coefficient of variation was calculated as $SD_{eEPSC}/Mean_{eEPSC}$ (Kullmann 1994). Statistical comparisons were made with the two-tailed unpaired t-test, one-way ANOVA, two-way ANOVA, or the Kolmogorov-Smirnov test as indicated. Differences with $p < 0.05$ were accepted as significant. No statistical method was used to predetermine sample sizes, but our sample sizes are similar to those generally used in the field. The normal distribution of the data was assessed by the Kolmogorov-Smirnov test. No test for outliers was applied. No data were excluded.

Results

1. Synaptotagmin-11 Inhibits Spontaneous Neurotransmission.

328 To investigate the function of Syt11 in spontaneous release, we used Syt11
329 knockout (KO) hippocampal neurons. Primary cultured hippocampal neurons from
330 floxed Syt11 knock-in mice were infected with cre-expressing lentivirus to generate
331 Syt11-KO neurons, while catalytically inactive Δcre served as a negative control. This
332 applies to all the KO experiments described here. The KO efficiency of Syt11
333 was >98%, while SNARE proteins involved in spontaneous release – syb2, vti1a, and
334 syntaxin1 – remained unaffected (Figure 1a, b). Next, we monitored the mEPSCs in
335 the presence of TTX and the $GABA_A$ receptor blocker bicuculline in control and
336 Syt11-KO neurons. The Syt11-KO neurons showed an increased average frequency of
337 spontaneous release by ~4-fold (Figure 1c, d). On the other hand, the mEPSC
338 amplitudes did not change significantly (Figure 1e), consistent with a previous report
339 (Shimojo *et al.* 2019). The membrane properties of Syt11-KO neurons did not differ
340 from controls, since the resting membrane potential and membrane resistance did not
341 significantly differ (Figure 1f, g). Interestingly, Syt11-KO greatly enhanced the
342 high-frequency spontaneous neurotransmission that occurred at lower inter-event
343 intervals (Figure 1h). The amplitudes of evoked EPSCs (eEPSCs) and coefficient of
344 variation in Syt-11 KO neurons did not significantly differ from controls (Figure 1i,
345 j), which supports a selective action of Syt11 in regulating spontaneous release.
346 When we overexpressed Syt11 by infecting hippocampal neurons with lentivirus
347 expressing Syt11 (Figure 2a, b), we found a significant decrease of mEPSC frequency
348 (Figure 2c, d). The overexpression (OE) level of Syt11 protein was ~1.7-fold that of
349 endogenous expression. Under this condition, the mEPSC amplitudes and membrane
350 properties were not affected (Figure 2e–g). All together, these results showed that
351 Syt11 suppresses spontaneous release under physiological conditions.
352
353 **2. Syt11 Directly Interacts with Vti1a.**
354 To understand the molecular mechanism of Syt11 inhibition in spontaneous
355 transmission, we searched for its interacting proteins using GST-Syt11 in pull-down
356 experiments in mouse brain extracts (Figure 3a). We found that vti1a was specifically
357 pulled down by Syt11 while syb2 and syntaxin1 failed to bind Syt11. Furthermore,

co-immunoprecipitation experiments with vti1a antibody showed that Syt11 was in the same complex with vti1a (Figure 3b). To test whether Syt11 binds vti1a directly, we purified His-tagged vti1a and incubated it with purified GST-Syt11 (Figure 3c). The result showed that Syt11 directly interacted with vti1a (Figure 3d).

To explore whether the Syt11-vti1a interaction occurs at synapses, we performed immunofluorescence experiments in hippocampal neurons expressing myc-Syt11 (Figure 3e). Syt11 was partially co-localized with endogenous vti1a in boutons, supporting its diverse functions in synaptic exocytosis and endocytosis (Wang *et al.* 2016).

3. Syt11 Inhibits Spontaneous Neurotransmission *via* Vti1a.

Since Syt11 specifically bound vti1a, which selectively functions in spontaneous release (Ramirez *et al.* 2012), we reasoned that Syt11 may regulate spontaneous neurotransmission by inhibiting vti1a. To test this hypothesis, we knocked down vti1a in Syt11-KO hippocampal neurons (Figure 4a, b). If vti1a is the main target of Syt11 regulation, knocking down vti1a should eliminate the increased frequency in Syt11-KO cells. Two different lentivirus-expressing shRNAs against vti1a both reduced its protein expression to ~50%, while a non-targeting shRNA served as the negative control. Indeed, vti1a knockdown (KD) by both shRNAs reversed the Syt11-KO phenotype by decreasing the frequency of mEPSCs, in particular the high-frequency events (Figure 4c–e). We also confirmed that vti1a-KD itself reduced the spontaneous release frequency, especially high-frequency events (Ramirez *et al.* 2012). Syt11-KO and vti1a-KD showed an average frequency and cumulative probability similar to vti1a-KD alone, indicating that vti1a is the main target of Syt11 regulation.

To validate that Syt11-vti1a selectively functions in spontaneous release, we monitored eEPSCs and sEPSCs (without TTX) from the same neurons (Figure 5). Paired-pulse stimulation at 50 ms (20 Hz), 100 ms (10 Hz), 200 ms (5 Hz), and 500 ms (2 Hz) intervals showed that paired-pulse ratios were unaffected in the absence of Syt11 and/or vti1a (Figure 5a–b), suggesting that Syt11 and vti1a do not function in

388 evoked release. On the other hand, sEPSCs recorded from the same cells after
389 paired-pulse stimulation showed similar phenotypes as the mEPSCs (Figure 5c, d *vs*
390 4c, d). Syt11-KO significantly increased sEPSC frequency while vti1a-KD reversed
391 the Syt11-KO phenotype. These results support the hypothesis that Syt11-vti1a
392 specifically modulates spontaneous release.
393
394 **4. Syt11 Interacts with Vti1a through Multiple Domains.**
395 To identify the domains required for Syt11 binding to vti1a, we constructed a
396 series of Syt11 truncation mutants that included its cytosolic domain (GST-Syt11), the
397 cytosolic domain without the linker, C2A, or C2B domain (GST-ΔLinker,
398 GST-ΔC2A, GST-ΔC2B), and the linker, C2A, and C2B domains alone (GST-Linker,
399 GST-C2A, GST-C2B, Figure 6a). Coomassie staining revealed the purity of these
400 mutants and those that included the linker region were more vulnerable to degradation
401 (Figure 6b). All these mutants bound vti1a to different extents. Among them, ΔC2A
402 displayed weaker binding than ΔC2B or ΔLinker while the C2A domain showed
403 stronger interaction than the C2B or Linker domain (Figure 6c). These results
404 revealed an important role of the C2A domain in the Syt11-vti1a interaction,
405 consistent with a previous report in which the C2A domain of Syt11 was shown to
406 bind vti1a more strongly than C2B (Milochau *et al.* 2014).
407
408 **5. C2A Domain Rescues Syt11-KO Phenotype.**
409 Since the C2A domain of Syt11 had a high binding affinity for vti1a and vti1a
410 was the main target of the Syt11 regulation of spontaneous release, we tested whether
411 the C2A domain by itself rescued the Syt11-KO phenotype similar to the full-length
412 (FL) protein. Lentivirus expressing Syt11 FL or Syt11 C2A was used in KO neurons
413 while GFP was used as the negative control (Figure 7a, b). As expected, Syt11-KO
414 increased the frequency of mEPSCs and both Syt11 FL and Syt11 C2A expression
415 largely rescued the phenotype both in average frequency and cumulative probability
416 (Figure 7a–c). Therefore, the C2A domain of Syt11 was sufficient to reverse the KO
417 phenotype. As no other binding proteins have been reported for the C2A domain of

418 Syt11 (Milochau *et al.* 2014), these results further supported our hypothesis that Syt11
419 inhibits spontaneous neurotransmission mainly through its interaction with vti1a.
420
421 **Discussion**
422 In this study, we identified Syt11 as a novel inhibitor of spontaneous
423 neurotransmission through its direct binding with vti1a. Knockout of endogenous
424 Syt11 in hippocampal neurons increased the frequency of spontaneous release events
425 while overexpression suppressed it (Figure 1, 2). The specific interaction of Syt11
426 with vti1a was revealed by GST pull-down, co-immunoprecipitation, purified protein
427 binding assays, and co-localization experiments (Figure 3). Importantly, the increased
428 spontaneous release in Syt11-KO neurons was reversed by vti1a KD, identifying vti1a
429 as the main target of Syt11 inhibition (Figure 4). Furthermore, we showed that Syt11
430 directly bound to vti1a through its C2A domain (Figure 6). Expression of the
431 full-length Syt11 protein or the C2A domain alone both rescued the Syt11-KO
432 phenotype, further supporting the hypothesis that Syt11 inhibits spontaneous
433 neurotransmission *via* vti1a (Figure 7).
434 Vti1a-containing vesicles are actively trafficked at rest and support spontaneous
435 neurotransmission (Ramirez *et al.* 2012). We showed here that Syt11 selectively
436 regulated vti1a-mediated spontaneous release since vti1a KD abolished the Syt11-KO
437 phenotype and Syt11 interacted with vti1a, but not syb2. In Syt11-KO terminals, the
438 frequency of mEPSCs increased ~4-fold. As both syb2- and vti1a-vesicles contributed
439 to spontaneous neurotransmission, this result suggested that the majority of
440 vti1a-containing vesicles (>75%) are “clamped” under physiological conditions.
441 Strikingly, Syt11-OE (at ~1.7-fold of the endogenous level) reduced mEPSC
442 frequency to ~1/3 of control. If we assume that all vti1a-vesicles are clamped under
443 this condition, these data suggest that vti1a-vesicles contribute to ~2/3 of spontaneous
444 release. It is possible that a compensation mechanism occurred in cultured
445 hippocampal neurons during the time of Syt11-KO or the overexpression process,
446 which lasted for 10–11 days. It remains to be determined whether acute manipulation
447 of Syt11 protein levels leads to even more severe phenotypes. Altogether, our results

point to a crucial role of vti1a in spontaneous neurotransmission and its precise regulation by Syt11 under physiological conditions. It would be interesting to investigate whether abnormal regulation of vti1a by Syt11 participates in brain diseases such as schizophrenia and Parkinson's disease, in which overexpression of Syt11 has been suggested (Huynh *et al.* 2003; Inoue *et al.* 2007; Wang *et al.* 2018). Given the diverse functions of vti1a in both spontaneous and evoked neurotransmission, as well as dense-core vesicle secretion (Ramirez *et al.* 2012; Kononenko & Haucke 2012; Walter *et al.* 2014; Crawford *et al.* 2017; Emperador-Melero *et al.* 2018; Emperador-Melero *et al.* 2019), a pathological expression level of Syt11 may lead to wide-ranging defects in cell-to-cell communication in the brain through the Syt11-vti1a interaction.

To date, vti1a is the only interactor identified for the C2A domain of Syt11 (Milochau *et al.* 2014). Its C2A domain also fails to bind phospholipids biochemically (von Poser *et al.* 1997). On the contrary, the C2A domain of Syt1 binds the SNARE complex and phospholipids in a Ca^{2+}-dependent manner (Pallanck 2003). The C2A domain of Syt4 shows 73% identity and 87% similarity with Syt11, while that of Syt1 shows 49% identity and 66% similarity. Syt4 regulates evoked and spontaneous neurotransmission similar to Syt11 (Dean *et al.* 2009). It is possible that Syt4, and perhaps other Syt members, also inhibits vti1a under resting conditions. Further studies are needed to map the binding site on the C2A domain of Syt11 and to understand whether vti1a is regulated by other Syt members and/or proteins. As the important roles of spontaneous neurotransmission are increasingly being revealed, it would be interesting to explore the regulation of molecularly distinct vesicles responsible for spontaneous release.

Acknowledgements

We greatly appreciate the kind help of Profs. Jianyuan Sun, Xiaofeng Yang, and Dr. Xuefeng Wang with the electrophysiological experiments, Prof. Deqiang Zheng with statistical analysis, and valuable comments on the manuscript by Profs. Jianyuan Sun and Weiping Han. This study was supported by grants from the National Natural

Science Foundation of China (31471085 to C.X.Z. 91849103 and 81671248 to R.L.), and the Beijing Natural Science Foundation Program and Scientific Research Key Program of Beijing Municipal Commission of Education (KZ201510025023 to C.X.Z).

Conflict of interest

The authors declare no conflict of interest.

Author contributions

CXZ, RL, and SZ conceived and designed the study, WRL, YLW, CL, PG, FFZ, and JCL performed experiments, WRL, YLW, and CL analyzed data, MH and SZ interpreted data, CXZ, WRL, and SZ wrote the manuscript.

References

Advani, R. J., Bae, H. R., Bock, J. B., Chao, D. S., Doung, Y. C., Prekeris, R., Yoo, J. S. and Scheller, R. H. (1998) Seven novel mammalian SNARE proteins localize to distinct membrane compartments. J Biol Chem 273, 10317-10324.

Andreae, L. C. and Burrone, J. (2018) The role of spontaneous neurotransmission in synapse and circuit development. J Neurosci Res 96, 354-359.

Antonin, W., Fasshauer, D., Becker, S., Jahn, R. and Schneider, T. R. (2002) Crystal structure of the endosomal SNARE complex reveals common structural principles of all SNAREs. Nat Struct Biol 9, 107-111.

Bacaj, T., Wu, D., Yang, X., Morishita, W., Zhou, P., Xu, W., Malenka, R. C. and Sudhof, T. C. (2013) Synaptotagmin-1 and synaptotagmin-7 trigger synchronous and asynchronous phases of neurotransmitter release. Neuron 80, 947-959.

Bal, M., Leitz, J., Reese, A. L., Ramirez, D. M., Durakoglugil, M., Herz, J., Monteggia, L. M. and Kavalali, E. T. (2013) Reelin mobilizes a VAMP7-dependent synaptic vesicle pool and selectively augments spontaneous neurotransmission. Neuron 80, 934-946.

508 Bento, C. F., Ashkenazi, A., Jimenez-Sanchez, M. and Rubinsztein, D. C. (2016) The
509 Parkinson's disease-associated genes ATP13A2 and SYT11 regulate
510 autophagy via a common pathway. Nat Commun 7, 11803.
511 Cornelisse, L. N., Tsivtsivadze, E., Meijer, M., Dijkstra, T. M., Heskes, T. and
512 Verhage, M. (2012) Molecular machines in the synapse: overlapping protein
513 sets control distinct steps in neurosecretion. PLoS Comput Biol 8, e1002450.
514 Crawford, D. C., Ramirez, D. M., Trauterman, B., Monteggia, L. M. and Kavalali, E.
515 T. (2017) Selective molecular impairment of spontaneous neurotransmission
516 modulates synaptic efficacy. Nat Commun 8, 14436.
517 Dean, C., Liu, H., Dunning, F. M., Chang, P. Y., Jackson, M. B. and Chapman, E. R.
518 (2009) Synaptotagmin-IV modulates synaptic function and long-term
519 potentiation by regulating BDNF release. Nat Neurosci 12, 767-776.
520 Du, C., Wang, Y., Zhang, F. et al. (2017) Synaptotagmin-11 inhibits cytokine
521 secretion and phagocytosis in microglia. Glia 65, 1656-1667.
522 Emperador-Melero, J., Huson, V., van Weering, J., Bollmann, C., Fischer von
523 Mollard, G., Toonen, R. F. and Verhage, M. (2018) Vti1a/b regulate synaptic
524 vesicle and dense core vesicle secretion via protein sorting at the Golgi. Nat
525 Commun 9, 3421.
526 Emperador-Melero, J., Toonen, R. F. and Verhage, M. (2019) Vti Proteins: Beyond
527 Endolysosomal Trafficking. Neuroscience 420, 32-40.
528 Fatt, P. and Katz, B. (1950) Some Observations on Biological Noise. Nature 166,
529 597-598.
530 Fatt, P. and Katz, B. (1952) Spontaneous subthreshold activity at motor nerve
531 endings. J Physiol 117, 109-128.
532 Fawley, J. A., Hofmann, M. E. and Andresen, M. C. (2014) Cannabinoid 1 and
533 transient receptor potential vanilloid 1 receptors discretely modulate evoked
534 glutamate separately from spontaneous glutamate transmission. J Neurosci 34,
535 8324-8332.
536 Fredj, N. B. and Burrone, J. (2009) A resting pool of vesicles is responsible for
537 spontaneous vesicle fusion at the synapse. Nat Neurosci 12, 751-758.

538 Geppert, M., Goda, Y., Hammer, R. E., Li, C., Rosahl, T. W., Stevens, C. F. and
539 Sudhof, T. C. (1994) Synaptotagmin I: a major Ca2+ sensor for transmitter
540 release at a central synapse. Cell 79, 717-727.
541 Glitsch, M. (2006) Selective inhibition of spontaneous but not Ca2+ -dependent
542 release machinery by presynaptic group II mGluRs in rat cerebellar slices. J
543 Neurophysiol 96, 86-96.
544 Gonzalez-Islas, C., Bulow, P. and Wenner, P. (2018) Regulation of synaptic scaling
545 by action potential-independent miniature neurotransmission. J Neurosci Res
546 96, 348-353.
547 Groemer, T. W. and Klingauf, J. (2007) Synaptic vesicles recycling spontaneously
548 and during activity belong to the same vesicle pool. Nat Neurosci 10, 145-147.
549 Groffen, A. J., Martens, S., Diez Arazola, R. et al. (2010) Doc2b is a high-affinity
550 Ca2+ sensor for spontaneous neurotransmitter release. Science 327,
551 1614-1618.
552 Hu, H., Wang, X., Li, C. et al. (2021) Loss of Dysbindin Implicates Synaptic Vesicle
553 Replenishment Dysregulation as a Potential Pathogenic Mechanism in
554 Schizophrenia. Neuroscience 452, 138-152.
555 Hua, Z., Leal-Ortiz, S., Foss, S. M., Waites, C. L., Garner, C. C., Voglmaier, S. M.
556 and Edwards, R. H. (2011) v-SNARE composition distinguishes synaptic
557 vesicle pools. Neuron 71, 474-487.
558 Huntwork, S. and Littleton, J. T. (2007) A complexin fusion clamp regulates
559 spontaneous neurotransmitter release and synaptic growth. Nat Neurosci 10,
560 1235-1237.
561 Huynh, D. P., Scoles, D. R., Nguyen, D. and Pulst, S. M. (2003) The autosomal
562 recessive juvenile Parkinson disease gene product, parkin, interacts with and
563 ubiquitinates synaptotagmin XI. Hum Mol Genet 12, 2587-2597.
564 Ikeda, K. and Bekkers, J. M. (2009) Counting the number of releasable synaptic
565 vesicles in a presynaptic terminal. Proc Natl Acad Sci U S A 106, 2945-2950.
566 Inoue, S., Imamura, A., Okazaki, Y., Yokota, H., Arai, M., Hayashi, N., Furukawa,
567 A., Itokawa, M. and Oishi, M. (2007) Synaptotagmin XI as a candidate gene

568 for susceptibility to schizophrenia. Am J Med Genet B Neuropsychiatr Genet
569 144B, 332-340.
570 International Parkinson Disease Genomics, C., Nalls, M. A., Plagnol, V. et al. (2011)
571 Imputation of sequence variants for identification of genetic risks for
572 Parkinson's disease: a meta-analysis of genome-wide association studies.
573 Lancet 377, 641-649.
574 Kaeser, P. S. and Regehr, W. G. (2014) Molecular mechanisms for synchronous,
575 asynchronous, and spontaneous neurotransmitter release. Annu Rev Physiol
576 76, 333-363.
577 Kavalali, E. T. (2015) The mechanisms and functions of spontaneous neurotransmitter
578 release. Nat Rev Neurosci 16, 5-16.
579 Kavalali, E. T. (2018) Spontaneous neurotransmission: A form of neural
580 communication comes of age. J Neurosci Res 96, 331-334.
581 Kononenko, N. L. and Haucke, V. (2012) Spontaneous neurotransmission: a SNARE
582 for the rest. Neuron 73, 3-5.
583 Kullmann, D. M. (1994) Amplitude fluctuations of dual-component EPSCs in
584 hippocampal pyramidal cells: implications for long-term potentiation. Neuron
585 12, 1111-1120.
586 Liu, H., Dean, C., Arthur, C. P., Dong, M. and Chapman, E. R. (2009) Autapses and
587 networks of hippocampal neurons exhibit distinct synaptic transmission
588 phenotypes in the absence of synaptotagmin I. J Neurosci 29, 7395-7403.
589 Mathew, S. S., Pozzo-Miller, L. and Hablitz, J. J. (2008) Kainate modulates
590 presynaptic GABA release from two vesicle pools. J Neurosci 28, 725-731.
591 Maximov, A., Shin, O. H., Liu, X. and Sudhof, T. C. (2007) Synaptotagmin-12, a
592 synaptic vesicle phosphoprotein that modulates spontaneous neurotransmitter
593 release. J Cell Biol 176, 113-124.
594 Maximov, A. and Sudhof, T. C. (2005) Autonomous function of synaptotagmin 1 in
595 triggering synchronous release independent of asynchronous release. Neuron
596 48, 547-554.
597 Milochau, A., Lagree, V., Benassy, M. N. et al. (2014) Synaptotagmin 11 interacts

598 with components of the RNA-induced silencing complex RISC in clonal
599 pancreatic beta-cells. FEBS Lett 588, 2217-2222.
600 Nishiki, T. and Augustine, G. J. (2004) Synaptotagmin I synchronizes transmitter
601 release in mouse hippocampal neurons. J Neurosci 24, 6127-6132.
602 Pallanck, L. (2003) A tale of two C2 domains. Trends Neurosci 26, 2-4.
603 Pang, Z. P., Bacaj, T., Yang, X., Zhou, P., Xu, W. and Sudhof, T. C. (2011) Doc2
604 supports spontaneous synaptic transmission by a Ca(2+)-independent
605 mechanism. Neuron 70, 244-251.
606 Pang, Z. P. and Sudhof, T. C. (2010) Cell biology of Ca2+-triggered exocytosis. Curr
607 Opin Cell Biol 22, 496-505.
608 Pang, Z. P., Sun, J., Rizo, J., Maximov, A. and Sudhof, T. C. (2006) Genetic analysis
609 of synaptotagmin 2 in spontaneous and Ca2+-triggered neurotransmitter
610 release. EMBO J 25, 2039-2050.
611 Pihlstrom, L., Axelsson, G., Bjornara, K. A. et al. (2013) Supportive evidence for 11
612 loci from genome-wide association studies in Parkinson's disease. Neurobiol
613 Aging 34, 1708 e1707-1713.
614 Pratt, K. G., Zhu, P., Watari, H., Cook, D. G. and Sullivan, J. M. (2011) A novel role
615 for {gamma}-secretase: selective regulation of spontaneous neurotransmitter
616 release from hippocampal neurons. J Neurosci 31, 899-906.
617 Raingo, J., Khvotchev, M., Liu, P. et al. (2012) VAMP4 directs synaptic vesicles to a
618 pool that selectively maintains asynchronous neurotransmission. Nat Neurosci
619 15, 738-745.
620 Ramirez, D. M., Khvotchev, M., Trauterman, B. and Kavalali, E. T. (2012) Vti1a
621 identifies a vesicle pool that preferentially recycles at rest and maintains
622 spontaneous neurotransmission. Neuron 73, 121-134.
623 Regehr, W. G. (2012) Short-term presynaptic plasticity. Cold Spring Harb Perspect
624 Biol 4, a005702.
625 Sara, Y., Virmani, T., Deak, F., Liu, X. and Kavalali, E. T. (2005) An isolated pool of
626 vesicles recycles at rest and drives spontaneous neurotransmission. Neuron 45,
627 563-573.

628 Schupp, M., Malsam, J., Ruiter, M., Scheutzow, A., Wierda, K. D., Sollner, T. H. and
629 Sorensen, J. B. (2016) Interactions Between SNAP-25 and Synaptotagmin-1
630 Are Involved in Vesicle Priming, Clamping Spontaneous and Stimulating
631 Evoked Neurotransmission. J Neurosci 36, 11865-11880.
632 Sesar, A., Cacheiro, P., Lopez-Lopez, M. et al. (2016) Synaptotagmin XI in
633 Parkinson's disease: New evidence from an association study in Spain and
634 Mexico. J Neurol Sci 362, 321-325.
635 Shimojo, M., Madara, J., Pankow, S., Liu, X., Yates, J., 3rd, Sudhof, T. C. and
636 Maximov, A. (2019) Synaptotagmin-11 mediates a vesicle trafficking pathway
637 that is essential for development and synaptic plasticity. Genes Dev 33,
638 365-376.
639 Sreetama, S. C., Takano, T., Nedergaard, M., Simon, S. M. and Jaiswal, J. K. (2016)
640 Injured astrocytes are repaired by Synaptotagmin XI-regulated lysosome
641 exocytosis. Cell Death Differ 23, 596-607.
642 Sudhof, T. C. and Rothman, J. E. (2009) Membrane fusion: grappling with SNARE
643 and SM proteins. Science 323, 474-477.
644 Sun, J., Pang, Z. P., Qin, D., Fahim, A. T., Adachi, R. and Sudhof, T. C. (2007) A
645 dual-Ca2+-sensor model for neurotransmitter release in a central synapse.
646 Nature 450, 676-682.
647 Takamori, S., Holt, M., Stenius, K. et al. (2006) Molecular anatomy of a trafficking
648 organelle. Cell 127, 831-846.
649 Truckenbrodt, S. and Rizzoli, S. O. (2014) Spontaneous vesicle recycling in the
650 synaptic bouton. Front Cell Neurosci 8, 409.
651 von Poser, C., Ichtchenko, K., Shao, X., Rizo, J. and Sudhof, T. C. (1997) The
652 evolutionary pressure to inactivate. A subclass of synaptotagmins with an
653 amino acid substitution that abolishes Ca2+ binding. J Biol Chem 272,
654 14314-14319.
655 Walter, A. M., Kurps, J., de Wit, H. et al. (2014) The SNARE protein vti1a functions
656 in dense-core vesicle biogenesis. EMBO J 33, 1681-1697.
657 Wang, C., Kang, X., Zhou, L. et al. (2018) Synaptotagmin-11 is a critical mediator of

parkin-linked neurotoxicity and Parkinson's disease-like pathology. Nat Commun 9, 81.

Wang, C., Wang, Y., Hu, M., Chai, Z., Wu, Q., Huang, R., Han, W., Zhang, C. X. and Zhou, Z. (2016) Synaptotagmin-11 inhibits clathrin-mediated and bulk endocytosis. EMBO Rep 17, 47-63.

Wierda, K. D. and Sorensen, J. B. (2014) Innervation by a GABAergic neuron depresses spontaneous release in glutamatergic neurons and unveils the clamping phenotype of synaptotagmin-1. J Neurosci 34, 2100-2110.

Williams, C. L. and Smith, S. M. (2018) Calcium dependence of spontaneous neurotransmitter release. J Neurosci Res 96, 335-347.

Xu, J., Mashimo, T. and Sudhof, T. C. (2007) Synaptotagmin-1, -2, and -9: Ca(2+) sensors for fast release that specify distinct presynaptic properties in subsets of neurons. Neuron 54, 567-581.

Xu, J., Pang, Z. P., Shin, O. H. and Sudhof, T. C. (2009) Synaptotagmin-1 functions as a Ca2+ sensor for spontaneous release. Nat Neurosci 12, 759-766.

Yan, S., Wang, Y., Zhang, Y. et al. (2020) Synaptotagmin-11 regulates the functions of caveolae and responds to mechanical stimuli in astrocytes. FASEB J 34, 2609-2624.

Yang, X., Cao, P. and Sudhof, T. C. (2013) Deconstructing complexin function in activating and clamping Ca2+-triggered exocytosis by comparing knockout and knockdown phenotypes. Proc Natl Acad Sci U S A 110, 20777-20782.

Figure legends

FIGURE 1 Knockout of Syt11 enhances spontaneous neurotransmission. (a and b) Representative Western blots (a) and quantification (b) of Syt11 protein expression levels in primary cultured hippocampal control neurons (Δcre) and Syt11-KO neurons (cre) (n = 3 independent cell culture preparations; error bars represent mean ± SEM; ****p <0.0001, Student's t-test). (c and d) Representative traces of mEPSCs (c) and average frequency (d) of control (0.55 ± 0.07 Hz, n = 28 cells/6 independent cell

culture preparations) and Syt11-KO neurons (1.94 ± 0.09 Hz, n = 24 cells/7 independent cell culture preparations) (mean ± SEM; ****p <0.0001). (e-g) Average amplitude (e) (50.19 ± 3.73 *vs* 45.89 ± 3.60 pA), resting membrane potential (f) (70.12 ± 3.42 *vs* 70.35 ± 3.65 mV), and membrane resistance (g) (116.20 ± 2.10 *vs* 119.10 ± 3.42 MΩ) of control and Syt11-KO neurons (mean ± SEM; n.s., not significant). (h) Average cumulative probability plot of mEPSC inter-event intervals of control and Syt11-KO neurons as in (d). Syt11 KO increased the high-frequency events (p <0.0001, Kolmogorov-Smirnov test). (i and j) Representative traces of eEPSCs (i) and average amplitude (j) of control (533.88 ± 133.03 pA, n = 11 cells/8 independent cell culture preparations) and Syt11-KO neurons (443.19 ± 87.07 pA, n = 12 cells/6 independent cell culture preparations) (mean ± SEM; n.s., not significant). The coefficient of variation for eEPSC amplitudes of control neurons is 0.28 ± 0.05, and that of Syt11-KO neurons is 0.22 ± 0.03. Both the eEPSC amplitudes and coefficients of variation show no significant difference in control and Syt11-KO neurons.

FIGURE 2 Overexpression of Syt11 decreases spontaneous neurotransmission. (a and b) Representative Western blots (a) and quantification (b) of Syt11 protein expression levels in primary cultured hippocampal control neurons (GFP) and Syt11-OE neurons (n = 3 independent cell culture preparations; error bars represent mean ± SEM; **p <0.01, Student's t-test). (c and d) Representative mEPSC traces (c) and average frequency (d) of control (0.54 ± 0.04 Hz, n = 18 cells/3 independent cell culture preparations) and Syt11-OE neurons (0.21 ± 0.03 Hz, n = 19 cells/3 independent cell culture preparations) (mean ± SEM; ****p <0.0001). (e-g) Average amplitude (e) (47.10 ± 3.08 *vs* 46.39 ± 3.62 pA), resting membrane potential (f) (71.12 ± 1.74 *vs* 73.75 ± 2.93 mV), and membrane resistance (g) (115.10 ± 3.64 *vs* 111.10 ± 3.70 MΩ) of control and Syt11-OE neurons (mean ± SEM; n.s., not significant). (h) Average cumulative probability of mEPSC inter-event intervals of control and Syt11-OE neurons as in (d). Syt11 OE decreased the high-frequency events (p <0.0001, Kolmogorov-Smirnov test).

FIGURE 3 Syt11 directly interacts with vti1a. (a) Western blots of GST pull-down experiments. Purified recombinant GST-Syt11 protein was incubated with mouse brain extract and bound proteins were detected with anti-vti1a, anti-Syb2, and anti-syntaxin1 antibodies (n = 3 independent cell culture preparations). (b) Western blots of co-immunoprecipitation of mouse anti-vti1a antibody with Syt11, while Syb2 and syntaxin1 were absent. Two percent of the mouse brain extract was loaded as input (n = 3 independent cell culture preparations). (c) SDS gels showing purified GST-Syt11 and GST visualized by Coomassie brilliant blue staining (n = 3 independent cell culture preparations). (d) GST pulldown with purified GST-Syt11 and His-vti1a (n = 3 independent cell culture preparations). (e) Confocal images showing hippocampal neurons expressing Myc-Syt11 stained with antibodies against Myc (green) and vti1a (red). Arrows indicate co-localized puncta at synapses (n = 3 independent cell culture preparations). Scale bar, 10 μm.

FIGURE 4 Syt11 inhibits spontaneous neurotransmission *via* vti1a. (a and b) Representative Western blots (a) and quantification (b) of vti1a protein expression levels in primary cultured hippocampal neurons infected with control (non-targeting shRNA, NT), vti1a KD-1, and vti1a KD-2 lentivirus (n = 3 independent cell culture preparations; error bars represent mean ± SEM; ***p <0.001, one-way ANOVA. (c and d) Representative traces of mEPSCs (c) and average frequency (d) in control (Δcre+ NT) (0.49 ± 0.04 Hz, n = 25 cells/4 independent cell culture preparations), Syt11-KO (cre + NT) (1.44 ± 0.05 Hz, n = 21 cells/5 independent cell culture preparations), vti1a-KD (Δcre + KD1 or KD2) (0.37 ± 0.04 Hz, n = 21 cells/5 independent cell culture preparations), and Syt11-KO/vti1a-KD (cre + KD1 or KD2) (0.38 ± 0.04 Hz, n = 21 cells/5 independent cell culture preparations) neurons (Mean ± SEM; ****p <0.0001, *p <0.05, two-way ANOVA). (e) Average cumulative probability of mEPSC inter-event intervals of control, Syt11-KO, vti1a-KD, and Syt11-KO/vti1a-KD neurons as in (d). Both vti1a-KD and Syt11-KO/vti1a-KD have fewer high-frequency events than controls (vti1a KD p = 0.0001, Syt11-KO/vti1a-KD

748 p <0.0001, Kolmogorov-Smirnov test).

749

750 FIGURE 5 Syt11 does not affect evoked neurotransmission. (a and c) Representative
751 eEPSC and sEPSC traces from the same cells (a). (b) Paired-pulse ratios in control
752 (1.34 ± 0.13, n = 19 cells/9 independent cell culture preparations; 1.06 ± 0.08, n = 23
753 cells/9 independent cell culture preparations; 0.97 ± 0.05, n = 26 cells/9 independent
754 cell culture preparations; 0.92 ± 0.07, n = 21 cells/9 independent cell culture
755 preparations), Syt11-KO (1.07 ± 0.13, n = 19 cells/9 independent cell culture
756 preparations; 0.92 ± 0.07, n = 20 cells/9 independent cell culture preparations; 1.04 ±
757 0.07, n = 24 cells/9 independent cell culture preparations; 0.95 ± 0.07, n= 19 cells/9
758 independent cell culture preparations), vti1a-KD (1.06 ± 0.13, n = 19 cells/9
759 independent cell culture preparations; 1.05 ± 0.07, n = 18 cells/9 independent cell
760 culture preparations, 1.02 ± 0.07, n=24 cells/9 independent cell culture preparations;
761 0.89 ± 0.07, n = 18 cells/9 independent cell culture preparations) and
762 Syt11-KO/vti1a-KD (1.10 ± 0.11, n = 26 cells/9 independent cell culture preparations;
763 0.93 ± 0.08, n = 22 cells/9 independent cell culture preparations; 0.93 ± 0.05, n = 30
764 cells/9 independent cell culture preparations; 0.78 ± 0.05, n = 20 cells/9 independent
765 cell culture preparations) neurons at 50 ms, 100 ms, 200 ms, and 500 ms
766 paired-stimulation, respectively (Mean ± SEM; two-way ANOVA). (d) Average
767 sEPSC frequency in control (0.56 ± 0.10 Hz, n = 19 cells/9 independent cell culture
768 preparations), Syt11-KO (1.70 ± 0.38 Hz, n = 20 cells/9 independent cell culture
769 preparations), vti1a-KD (0.41 ± 0.13 Hz, n = 19 cells/9 independent cell culture
770 preparations), and Syt11-KO/vti1a-KD (0.92 ± 0.21 Hz, n = 20 cells/9 independent
771 cell culture preparations) neurons (Mean ± SEM; **p <0.01, *p <0.05, two-way
772 ANOVA). (e) Average sEPSC amplitude in control (23.00 ± 1.80 pA, n = 19 cells/9
773 independent cell culture preparations), Syt11-KO (25.65 ± 1.21 pA, n = 20 cells/9
774 independent cell culture preparations), vti1a-KD (23.11 ± 1.16 pA, n = 19 cells/9
775 independent cell culture preparations), and Syt11-KO/vti1a-KD (22.80 ± 0.81 pA, n =
776 20 cells/9 independent cell culture preparations) neurons (Mean ± SEM; two-way
777 ANOVA). Paired-pulse ratios are unaffected in the absence of Syt11 and/or vti1a

while sEPSCs are affected similarly to mEPSCs.

FIGURE 6 Syt11 interacts with vti1a through multiple domains. (a) Schematic of GST-Syt11 and GST-Syt11 truncations (solid lines, amino-acids included; dashed lines, deletions). (b) Purified GST-Syt11 and its mutants visualized by Coomassie brilliant blue staining of SDS gels (n = 4 independent cell culture preparations). (c) Western blots of GST pull-down with purified GST-Syt11, its mutations, and His-vti1a (n = 4 independent cell culture preparations).

FIGURE 7 The C2A domain rescues the Syt11-KO phenotype. (a and b) Representative mEPSC traces (a) and average frequency (b) of control (Δcre + GFP) (0.53 ± 0.04 Hz, n = 25 cells/5 independent cell culture preparations), Syt11-KO (cre + GFP) (2.02 ± 0.12 Hz, n = 26 cells/5 independent cell culture preparations), and Syt11-KO neurons infected with Syt11 FL (0.81 ± 0.05 Hz, n = 26 cells/6 independent cell culture preparations) or Syt11 C2A lentivirus (0.77 ± 0.05 Hz, n = 21 cells/5 independent cell culture preparations) (mean ± SEM; ****p <0.0001, one-way ANOVA). (c) Average cumulative probability of mEPSC inter-event intervals in control, Syt11-KO, and Syt11-KO neurons infected with Syt11 FL or Syt11 C2A as in (b). Both Syt11 FL and Syt11 C2A significantly reverse the Syt11 KO phenotype (Syt11 FL p <0.0001, Syt11 C2A p <0.0001, Kolmogorov-Smirnov test).

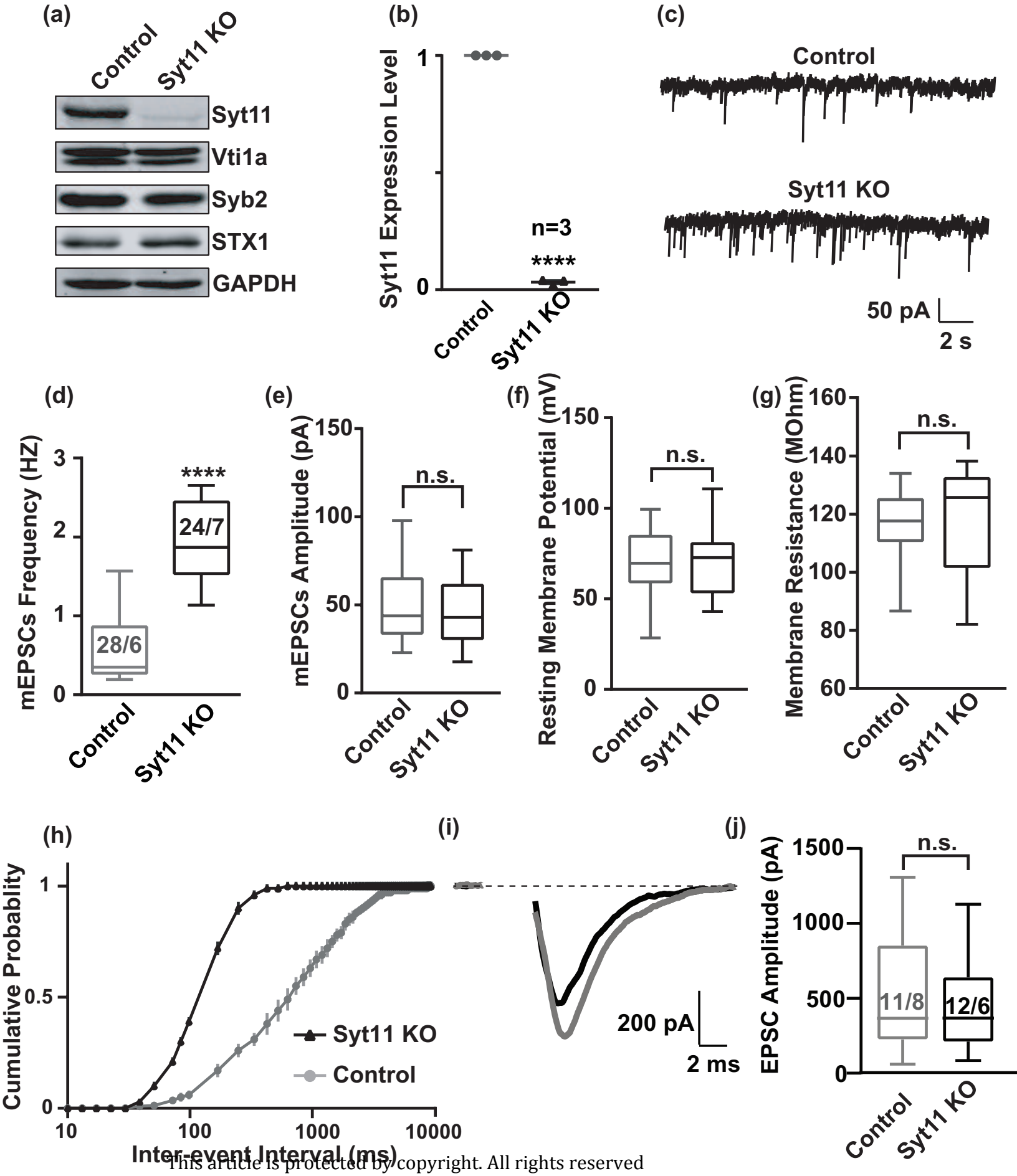

jnc_15523_f1.eps

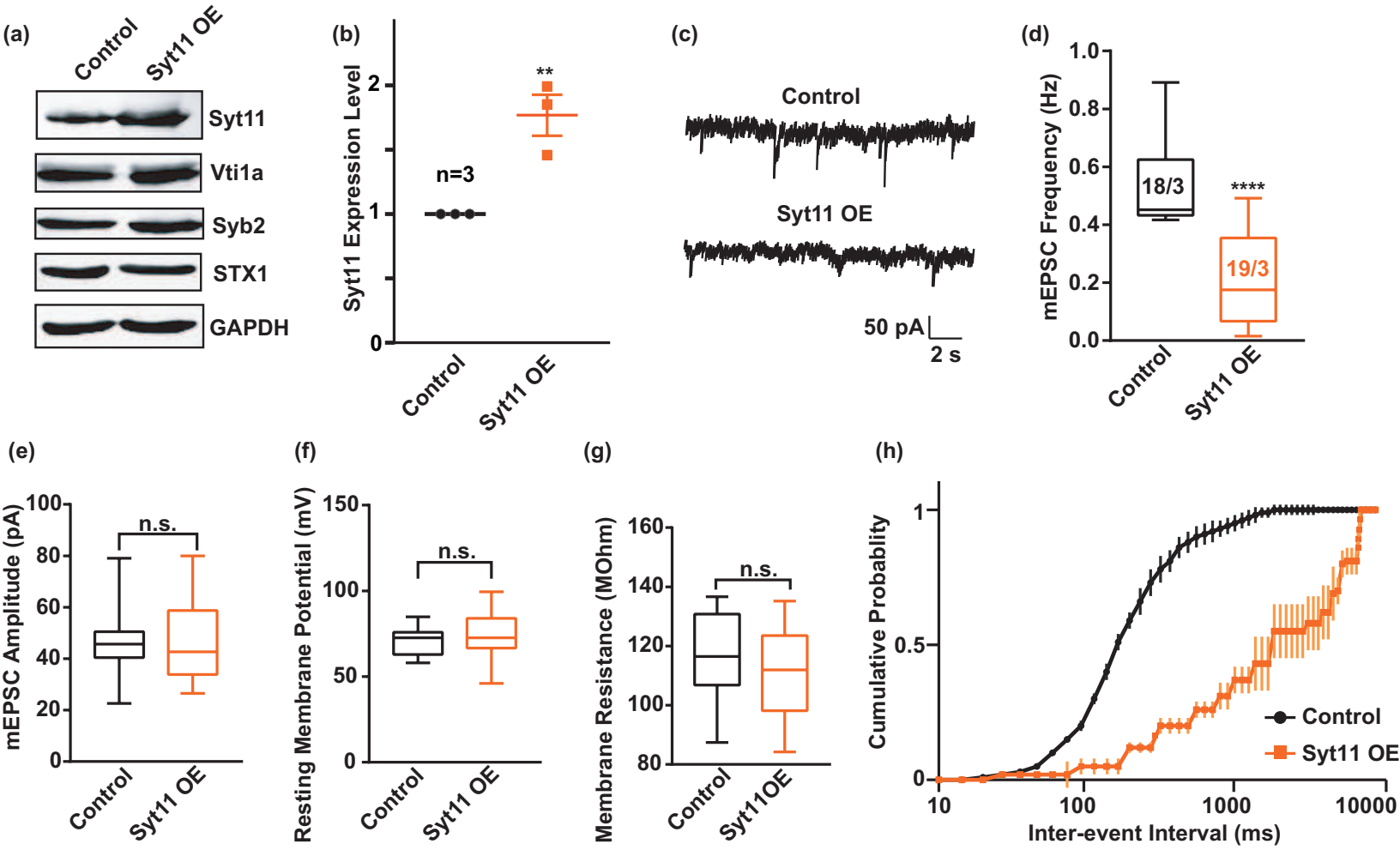

jnc_15523_f2.eps

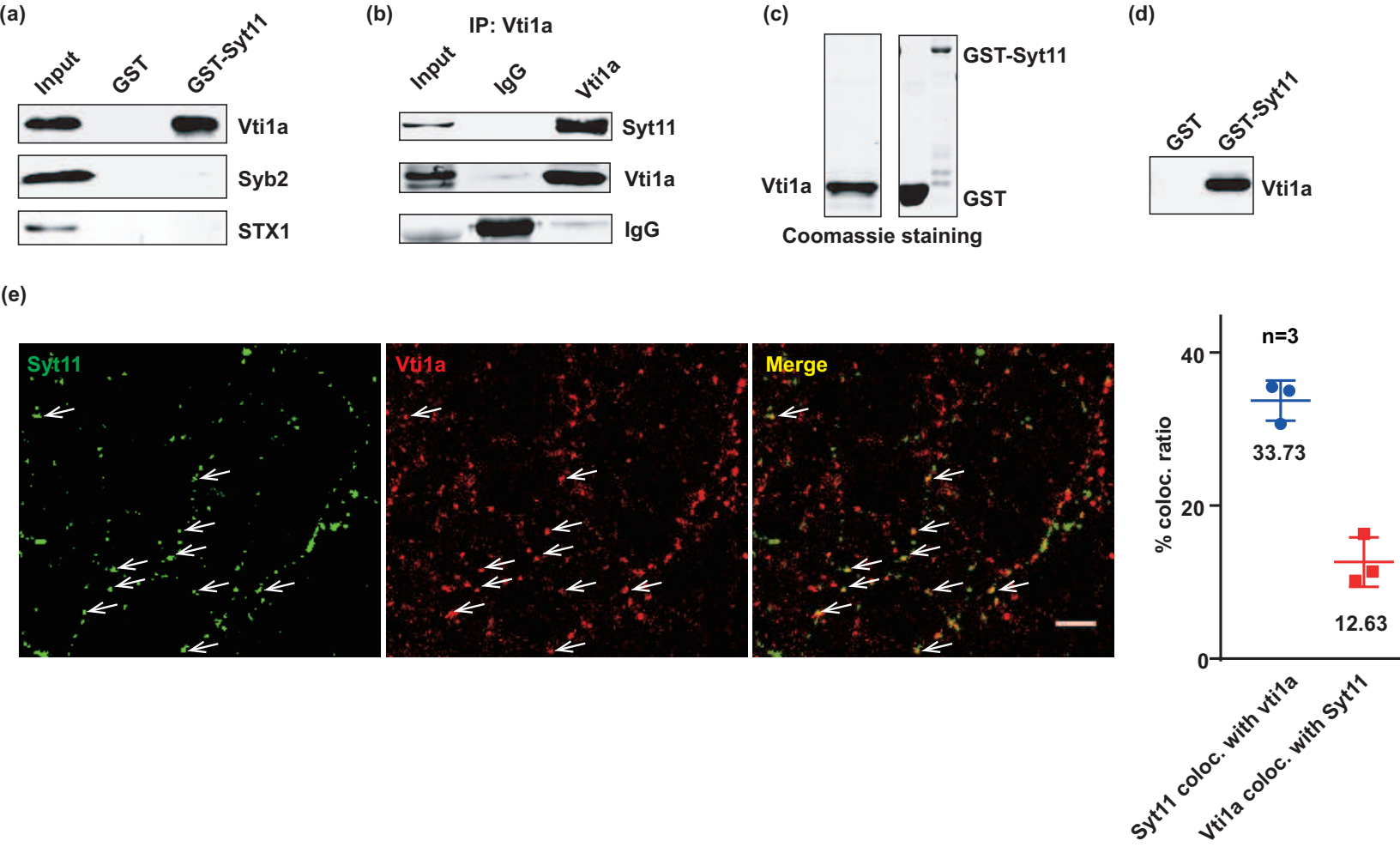

jnc_15523_f3.eps

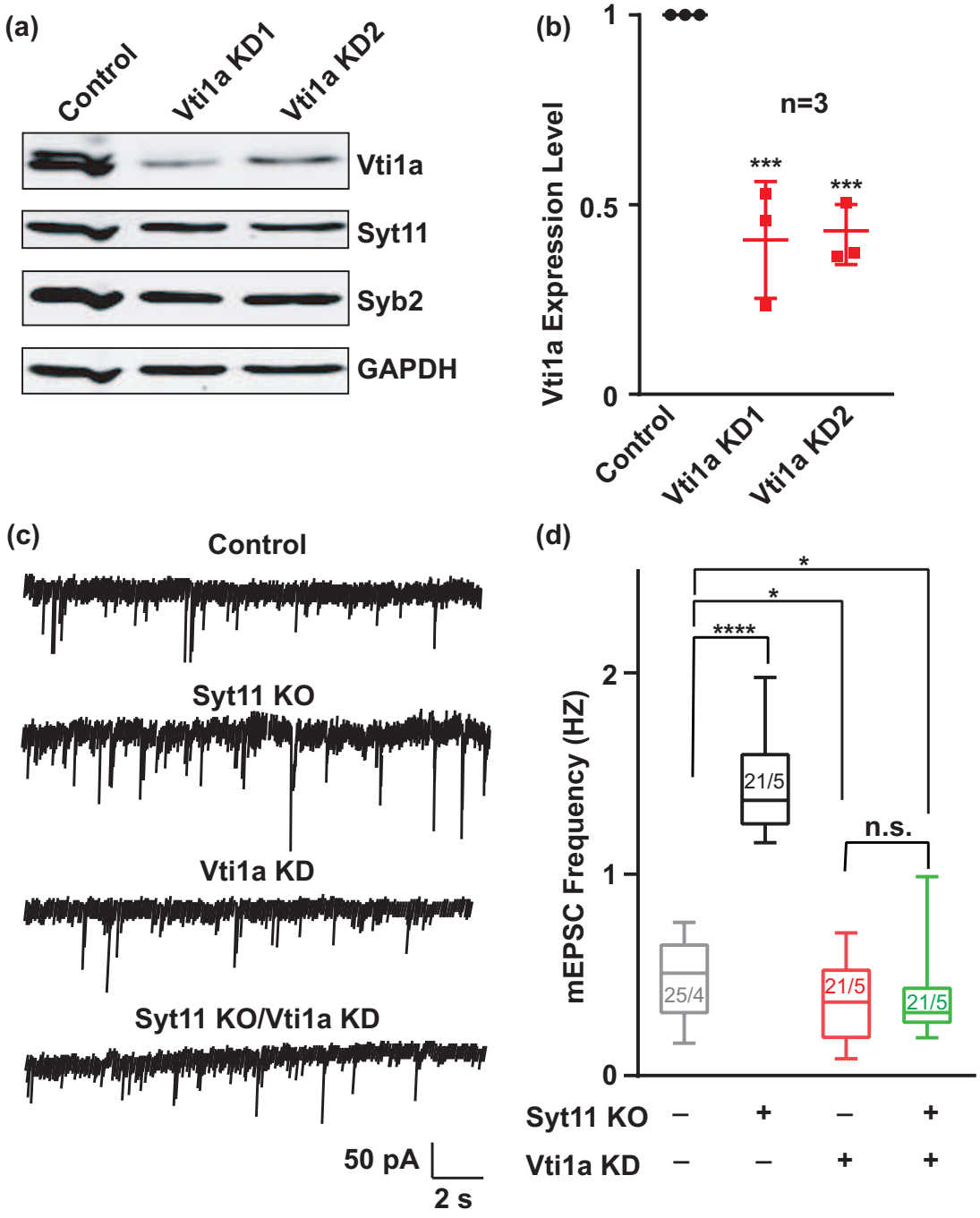

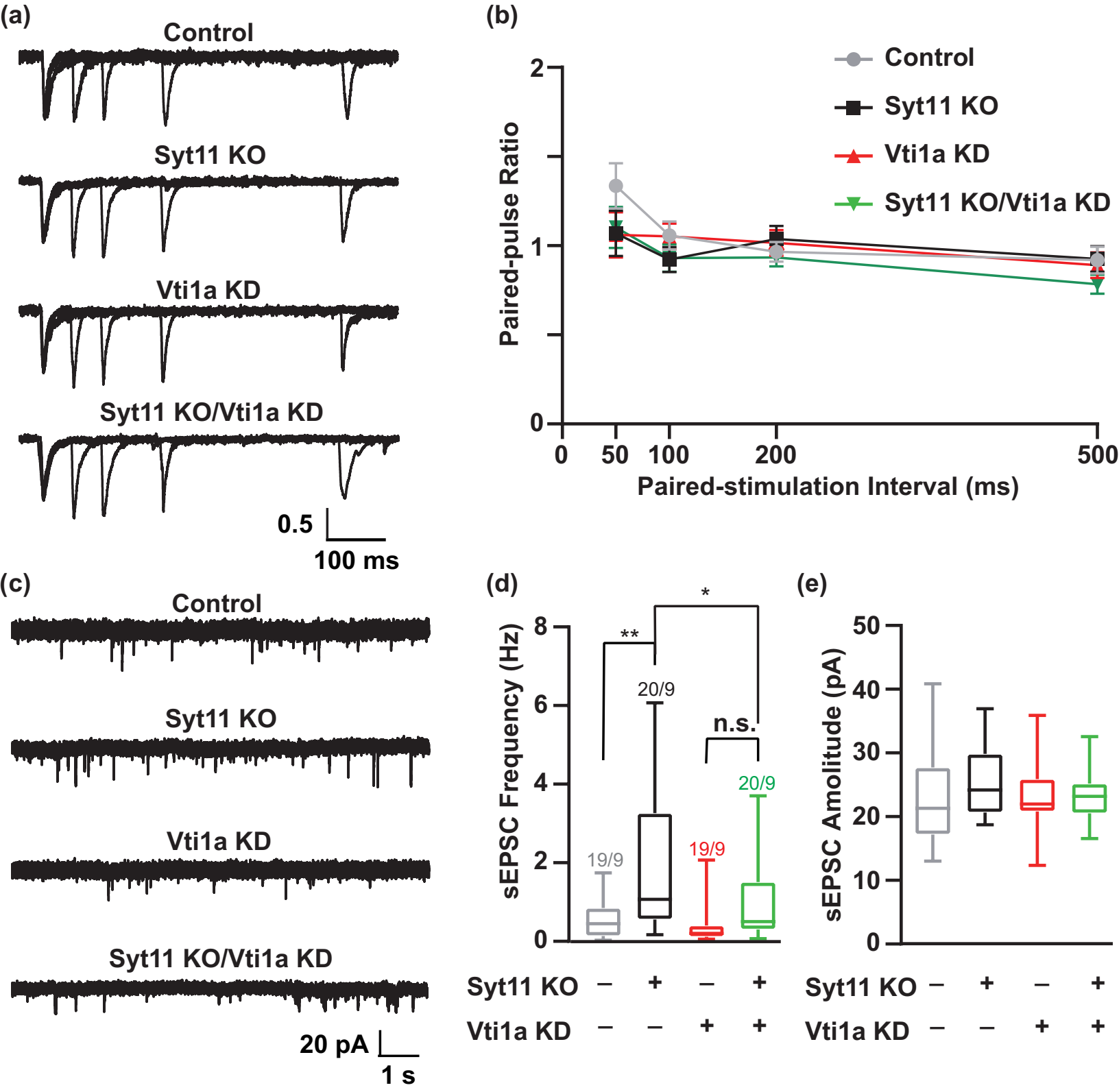

jnc_15523_f5.eps